

Homophily Based on Few Attributes Can Impede Structural Balance


Piotr J. Górski¹, Klavdiya Bochenina², Janusz A. Hołyst^{1,2} and Raissa M. D'Souza^{3,4,*}

¹*Faculty of Physics, Warsaw University of Technology, Koszykowa 75, PL 00-662 Warsaw, Poland*

²*ITMO University, Kronverkskiy avenue 49, RU 197101 Saint Petersburg, Russia*

³*University of California, Davis, California 95616, USA*

⁴*Santa Fe Institute, Santa Fe, New Mexico 87501, USA*

 (Received 24 January 2020; revised 15 June 2020; accepted 9 July 2020; published 13 August 2020)

Homophily between agents and structural balance in connected triads of agents are complementary mechanisms thought to shape social groups leading to, for instance, consensus or polarization. To capture both processes in a unified manner, we propose a model of pair and triadic interactions. We consider N fully connected agents, where each agent has G underlying attributes, and the similarity between agents in attribute space (i.e., homophily) is used to determine the link weight between them. For structural balance we use a triad-updating rule where only one attribute of one agent is changed intentionally in each update, but this also leads to accidental changes in link weights and even link polarities. The link weight dynamics in the limit of large G is described by a Fokker-Planck equation from which the conditions for a phase transition to a fully balanced state with all links positive can be obtained. This “paradise state” of global cooperation is, however, difficult to achieve requiring $G > O(N^2)$ and $p > 0.5$, where the parameter p captures a willingness for consensus. Allowing edge weights to be a consequence of attributes naturally captures homophily and reveals that many real-world social systems would have a subcritical number of attributes necessary to achieve structural balance.

DOI: [10.1103/PhysRevLett.125.078302](https://doi.org/10.1103/PhysRevLett.125.078302)

Introduction.—Understanding human behavior is a fundamental challenge and models from physics can provide quantitative frameworks for analyzing social dynamics [1], with recent advances in understanding the phenomena of social polarization, segregation and consensus (e.g., Refs. [2–5]). Given the current need for encouraging the adoption of social norms that promote public health [6,7], first-principles models that provide rigorous underpinnings to how opinions evolve are more relevant than ever. Opinions, preferences, actions (or generally attributes) of humans are not independent variables but they are a part of and rely on the other members of a social network. Recent experiments and analysis show that social networks are influenced by a set of distinct processes with possibly competing interactions [8], with two of the most important being structural balance and homophilic relations between agents. Structural balance (also called Heider balance or social balance) considers links between a set of three agents and assumes that triadic interactions would lead towards eliminating tensions, finally producing a balanced triad [9–18]. Using this principle, Antal *et al.* [13] introduced a now seminal link-evolution model of local triad dynamics (LTD). They showed the existence of a phase transition from a quasistationary state to a “paradise” state (with full structural balance and no negative links). The LTD model is formulated at the level of link polarity (i.e., whether the link weight is positive or negative). We consider a more basic notion, that agents have a set of underlying attributes which

give rise to the link weights and that these coevolve towards structural balance. Thus we build a hybrid model with two-body interactions and three-body interactions, the latter of which are used in different branches of physics [19–22].

Existing coevolution models [23–30] study reaching the states of polarization and segregation by assigning scalar (usually binary) polarities to links and at most two-dimensional attributes to nodes. Instead, following the Axelrod model of culture dissemination [1,31,32], we assume that each of N agents possesses G categorical Boolean attributes and that edge weights decrease with increasing distance between agents in the G -dimensional attribute space. We introduce an attribute-based local triad dynamics (ABLTD) model, where rather than changing the polarity of a link in attempt to increase structural balance, a more fine-grained change is made and one underlying attribute of one agent is changed. In the large G and N limit the link weight dynamics can be described by a Fokker-Planck equation from which we show that the phase transition observed by Antal *et al.* occurs for $G > O(N^2)$. For most real systems, the number of known attributes would be subcritical and the system would not be able to achieve full balance and global cooperation. Allowing edge weights to depend on underlying attributes captures the perspective that the relations between people are dependent on the people themselves [33,34]. Moreover, it lets us rigorously unify the principles of homophily and of social balance and analyze the thermodynamic limit. This reveals

that homophily with only few attributes can prevent structural balance.

Model.—We consider a complete undirected signed network with no self-loops of N agents labeled $i = 1, 2, \dots, N$. Each agent's state is described by a G -dimensional vector of Boolean attributes $\mathbf{A}_i = \{a_i^g\}$ where $g = 1, 2, \dots, G$ as in Refs. [1,31,32]. Each attribute a_i^g is initially assigned $+1$ or -1 with equal probability. The attributes correspond to agents' opinions or preferences about G distinct subjects and can change in time. This allows a natural embedding in a Hamming space with $x_{ij} = (1/2G)\mathbf{A}_i^T \cdot \mathbf{A}_j$ denoting the transformed distance between agents i and j , and the polarity of their relation $P_{ij} = \text{sgn}(x_{ij}) \in \{\pm 1\}$. It follows that P_{ij} is positive (negative) if more than half of the attributes of nodes i and j are the same (different). To ensure having signed polarities we consider only odd numbers of attributes. The triad of agents is said to be *balanced* if the product of polarities of its three links is positive, i.e., $P_{ij}P_{jm}P_{mi} = 1$. Following Ref. [13], all triads can be classified by a type Δ_k ($k = 0, 1, 2, 3$), where k is the number of negative links contained. Unbalanced triads are of types Δ_1 and Δ_3 . Changing the polarity of one of a triad's links changes an unbalanced triad to a balanced one, and vice versa.

With this in place, we define the ABLTD dynamics. In each step a link in a random unbalanced triad $\Delta(ijm)$ is picked. For a triad of type Δ_3 a random link is chosen since the triad is symmetric. For a type Δ_1 with probability p the negative link is chosen and with probability $(1 - p)$ one of the positive links is chosen. We flip one attribute of one of triad's nodes (e.g., a_i^g) so that the chosen link's weight is shifted by $+\frac{1}{G}$ if it is a negative link that we want to turn positive, and by $-\frac{1}{G}$ if it is a positive link we want to turn negative. The larger the value of p the more likely that the negative link is chosen and driven towards a positive value. Hence p represents the eagerness of agents in an unbalanced Δ_1 triad to achieve consensus, i.e., to change negative links to positive ones instead of positive ones to negative. The coevolution of all three levels of the system's structure (attributes, links, and triads) is depicted in Fig. 1.

Asymptotic analytical solutions.—Every state of the system has a specific placement of agents at points of Hamming space. Because of indistinguishability of agents many such states are equivalent. For any given state one can in principle calculate the transition probabilities to all other states and with those probabilities calculate exact measures of balanced states. However, the number of possible states grows rapidly with N and G making the method infeasible in general.

For numerical simulations of a sufficiently large network after a number of updates one can observe the following states: (a) a stationary, paradise solution where only triads Δ_0 exist, (b) a stationary, nonparadise solution where balanced triads Δ_0 and Δ_2 exist, or (c) a quasistationary

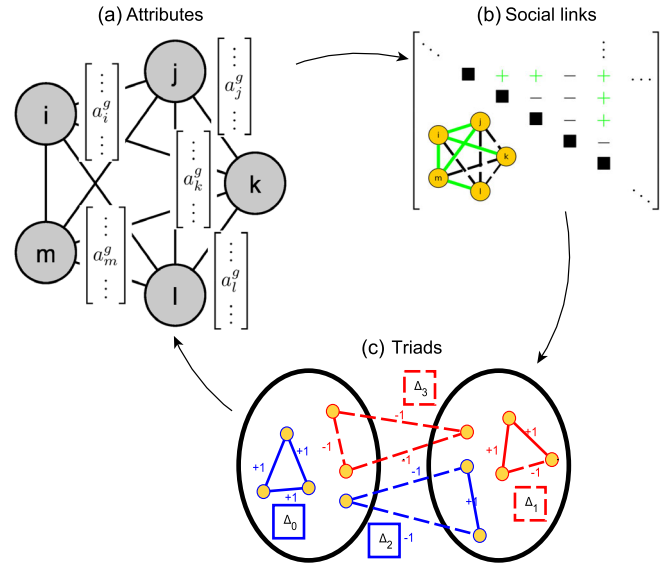


FIG. 1. Coevolution of attributes, edge polarities and triadic relations. Nodes' attributes (a) determine the relations between agents (b) and formation of balanced and unbalanced triads (c). Unbalanced triads drive the evolution of node attributes (a) and so on. In (b) positive and negative links are denoted with $+$ and $-$, respectively. Panel (c) emphasizes the four types of possible triads (without presenting all links): two balanced (Δ_0 and Δ_2) and two unbalanced (Δ_1 and Δ_3) denoted with blue and red colors, respectively. If only Δ_0 and Δ_2 were present a group polarization would be observed, i.e., agents could be divided into two hostile groups (marked with ellipses) with all links within members of the given group positive and with cross-links negative. However, having some unbalanced triads such a division does not exist.

solution where all types of triads coexist. Networks of type (c) are observed frequently and, although being unbalanced, they can be characterized by the approximately constant values of average measures such as positive link density ρ or triad densities (see Fig. 2 inset). These measures show fluctuations that lead finite-sized networks to ultimately reach one of the balanced solutions (a) or (b). The size of these fluctuations decrease with N and vanish with $N \rightarrow \infty$, meaning that in the thermodynamic limit a system will stay in a quasistationary state never reaching a balanced solution.

The possible values of the edge weights x_{ij} (from now on denoted simply as x) form a discrete set: $\mathbb{D} = \{-0.5, -0.5 + 1/G, -0.5 + 2/G, \dots, 0.5\}$. Any change in link weight is in increments $\pm 1/G$. Consider a random walk on \mathbb{D} . Let “jumping right” denote changing the weight to be closer to 0.5 and “jumping left” changing the weight to be closer to -0.5 with respective probabilities denoted r and l . During an update a walker stays in place with probability $1 - (r + l)$. There are two possible reasons of each jump: intentional and accidental. Intentional changes (ICs) are a desired consequence of the model dynamics and push triads towards structural balance. However, flipping an attribute

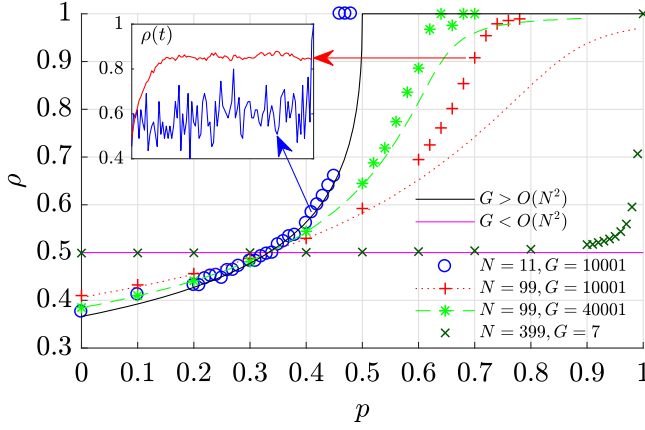


FIG. 2. Steady states of the ABLTD model for different relations between numbers of attributes G and nodes N . Shown is the density of positive links ρ as a function of probability p (desire for consensus). When $G > O(N^2)$ the system displays a transition to the paradise state ($\rho = 1$) provided p is sufficiently large. Analytical solutions (dashed and solid lines) fit the numerical results (markers) well for $p < 0.5$. Letting $G = O(N^\gamma)$ we see the fit is more accurate when γ is larger. The solid black and magenta curves show the solutions in the asymptotic limit $N \rightarrow \infty$ when $\gamma > 2$ and $\gamma < 2$, respectively. The inset shows time evolution for two example systems. Both achieve a quasistationary phase, after which the smaller system ultimately reaches the paradise state. Main plot shows the time and ensemble average of the link density when the system is in the quasistationary state if such a state is observed.

of one agent alters the weights of all this agent's links, not only the one that was intended. All these other $N - 2$ changes are accidental. An accidental change (AC) may result in a jump in either direction but with different probabilities dependent on the weight x . The jump probabilities can be easily calculated. For instance, probability of “jumping right”: $r \equiv P(r) = P(r|\text{AC})P(\text{AC}) + P(r|\text{IC})P(\text{IC})$. The full expressions (see Supplemental Material [35]) are

$$r(x) = \begin{cases} (0.5 - x)a_+ & \text{for } x > 0 \\ (0.5 - x)a_- + i_- & \text{for } x < 0 \end{cases}, \quad (1)$$

$$l(x) = \begin{cases} (0.5 + x)a_+ + i_+ & \text{for } x > 0 \\ (0.5 + x)a_- & \text{for } x < 0 \end{cases}, \quad (2)$$

where coefficients a_\pm and i_\pm represent probabilities $P(\text{AC}|x \geq 0)$ and $P(\text{IC}|x \geq 0)$, respectively, and in the mean-field approximation can be calculated as functions of N , p , and the density of positive links ρ (see Ref. [35]).

Assuming $G \rightarrow \infty$ the evolution of the probability that a link has a weight x , denoted $W(x, t)$, is described by the Fokker-Planck equation,

$$\frac{\partial W(x, t)}{\partial t} = \left[-\frac{\partial}{\partial x} c(x) + \frac{\partial^2}{\partial x^2} D(x) \right] W(x, t), \quad (3)$$

with drift $c(x) \propto r - l$ and diffusion $D(x) \propto r + l$ [36–38]. The quasistationary solution of Eq. (3) can be expressed by the corresponding potential as $W_{\text{st}}(x) \propto e^{-\phi(x)}$, where

$$\phi(x) = \frac{2G}{a_\pm + i_\pm} (a_\pm x^2 + i_\pm |x|). \quad (4)$$

This allows us to derive an equation for the quasistationary values of positive link density ρ , as $\rho = \int_{x>0} W_{\text{st}}(x) dx$. The right-hand side transforms into the transcendental function containing the cumulative standard normal distribution Φ dependent on ρ , p and the ratio (G/N^2) , see Supplemental Material [35] for details. Analytical solutions and numerical results for $N = 11, 99$, and 399 are shown in Fig. 2. The analytical fit is better for $p < 0.5$ and when (G/N^2) is larger. One can observe a phase transition in ρ that approaches 1 when the parameter p crosses a critical value dependent on N and G .

When $N \rightarrow \infty$ the density ρ is dependent on the relation between N and G as a solution of

$$\rho = \frac{\Phi_+}{\Phi_+ + \exp\left(\frac{G}{N^2} \frac{C_-^2 - C_+^2}{2}\right) \Phi_-}, \quad (5)$$

where $\Phi_\pm = \Phi(-C_\pm(\sqrt{G}/N))$ and C_\pm are rational functions of ρ and p (see Ref. [35]).

To quantify the study, let us assume $G = O(N^\gamma)$. There are three scenarios. (i) If $\gamma < 2$, then Eq (5) transforms into simply $\rho = 0.5$, where the quasistationary state with an equal number of positive and negative links exists. (The magenta line in Fig. 2.) It can be shown that the numbers of balanced and unbalanced triads are equal. (ii) If $\gamma > 2$, then using L'Hospital's rule we obtain $\rho = C_-/(C_+ + C_-)$, which can be transformed into

$$(\rho - 1)[(6p - 2)\rho^2 - 2\rho + 1] = 0. \quad (6)$$

The solutions are the paradise state $\rho = 1$ and a quasistationary solution $\rho = [1 + \sqrt{3(1 - 2p)}]^{-1}$ (the black line in Fig. 2). Thus for $\gamma > 2$ the ABLTD model is equivalent to the LTD model where a phase transition is observed at $p = 0.5$. Below $p < 0.5$ the system fluctuates around a quasistationary state. For $p > 0.5$, the system achieves paradise. Numerical simulations on even small systems show a qualitatively similar transition (e.g., $N = 11$, the blue dots, in Fig. 2). For such small systems sizes quasistationary fluctuations in ρ may be difficult to observe and the transition occurs for values $p < 0.5$.

The system phase diagram obtained for $N \rightarrow \infty$ is presented in Fig. 3. Apart from the already mentioned transition to paradise for $\gamma > 2$ it also emphasizes the transition for $\gamma = 2$, where the relation between numbers of nodes and attributes determines the system fate.

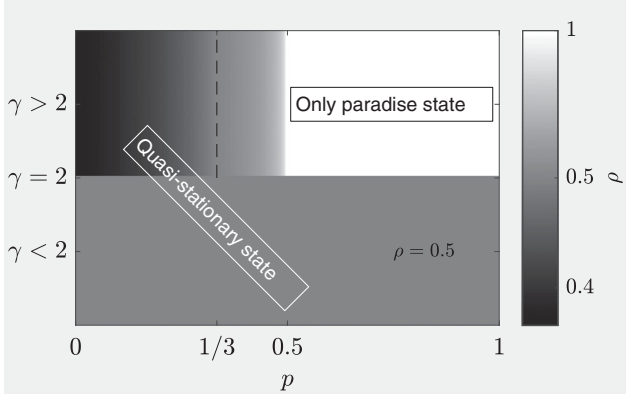


FIG. 3. Phase diagram for the ABLTD model in the asymptotic limit emphasizes the abrupt change of phases in $\gamma = 2$. Axes represent probability p and exponent γ , which describe agents' willingness for consensus and relation between numbers of nodes N and attributes G [$G = O(N^\gamma)$], respectively. The brightness represents the expected density of positive links ρ . When $\gamma > 2$ and $p \geq 0.5$ the only possible state is a paradise state ($\rho = 1$). Otherwise the system reaches the quasistationary state. For $\gamma < 2$ for all p the densities of positive and negative links are equal ($\rho = 0.5$) as are the number of balanced and unbalanced triads. For $\gamma > 2$ such equality is obtained for $p = 1/3$ (marked by a dashed line).

The final scenario is (iii) if $\gamma = 2$, then the system reaches an intermediate asymptotic solution (see Ref. [35]). Assuming $G = (bN)^2$ we obtain the equation for the critical point p^* , above which the quasistationary state disappears:

$$\frac{1}{\sqrt{2\pi}} \exp\left(-\frac{1}{2}b^2(1-p^*)^2\right) = bp^*\Phi(-b(1-p^*)). \quad (7)$$

The critical point and, therefore, the phase transition to paradise exist so long as $b \geq \sqrt{(2/\pi)}$.

No transition in three-node network.—With a very small number of nodes and/or attributes it is difficult to observe a quasistationary state. However, in such systems a finite state can be analyzed thoroughly. This allows for the observation of a different kind of transition than described previously: a transition where the change of parameter p alters the fate of a system from never to always reaching a paradise state, i.e., from $P_p = 0$ to $P_p = 1$, where P_p denotes the probability of paradise in the final state (see Fig. 4).

The simplest case is a network comprising only one triad. For such a system with a small number of attributes it is possible to calculate exactly the probabilities of stationary balanced states. With higher G , one needs numerical simulations, and with $G \rightarrow \infty$ analytical calculations are again possible. In such a case and assigning attributes at random, the initial distribution of triads of types Δ_0 , Δ_1 , Δ_2 , and Δ_3 is equal to $\frac{1}{8}$, $\frac{3}{8}$, $\frac{3}{8}$, and $\frac{1}{8}$. Still, the attribute update

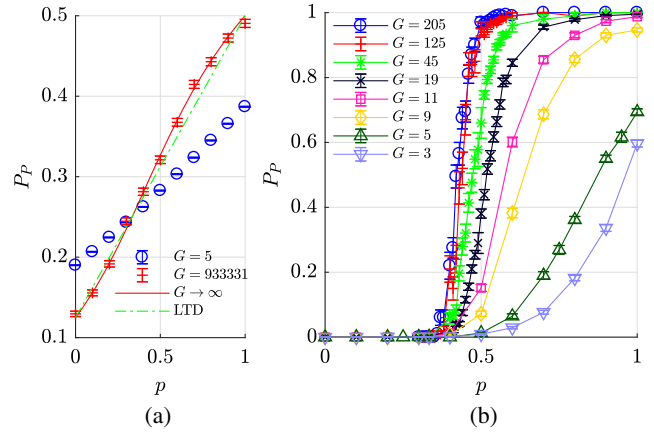


FIG. 4. Observed transitions of fates for small systems of size (a) $N = 3$ and (b) $N = 11$. Plots show the probability of reaching paradise P_p in ABLTD as a function of incentive to achieve consensus p . (a) In the case of a one-triad system there is no transition. The figure compares P_p for the numerical results of two diverse numbers of attributes G and the approximate $P_p(p)$ in the limit $G \rightarrow \infty$. Numerical results for large G agree with the analytical solution. The expected analytical results for the LTD model are also shown for comparison. (b) In the system with $N = 11$ the transition from never ($P_p = 0$) to always ($P_p = 1$) reaching paradise is observed and becomes sharper with increasing G .

causes two links to change their weights, but since $G \rightarrow \infty$ the probability of crossing the polarity change threshold (i.e., $x = 0$) for both of the links at the same time is negligible. Thus, with one edge flip a triad of type Δ_3 always turns into Δ_2 . The fate of a triad of type Δ_1 depends on the parameter p . The evolution of weights for links in such a triad is given as follows:

$$\dot{x}_- = p - (1-p)x_-, \quad (8)$$

$$\dot{x}_+ = -\frac{1-p}{2} - \frac{1+p}{2}x_+, \quad (9)$$

where x_{\pm} represents the weight of one of the two positive links or a negative link in this triad. Additive constant terms in Eqs. (8)–(9) are related to the intentional change of a corresponding link, while the linear parts to the accidental change of an adjacent link. These equations are valid up to the moment when any of the link weights cross 0, which is equivalent to the flip of the link polarity.

Probability of a change $\Delta_1 \rightarrow \Delta_0$ is equivalent to calculating the probability that a negative link will be first to change polarity. Equations (8)–(9) let us calculate $P_{\Delta_1 \rightarrow \Delta_0}$ (see Supplemental Material [35] for details) and derive an asymptotic probability of reaching the paradise state: $P_p(p) = \frac{1}{8} + P_{\Delta_1 \rightarrow \Delta_0}(p)\frac{3}{8}$. The results for numerical simulations averaged over initial conditions and an asymptotic solution as well as the results for the LTD model are presented in Fig. 4(a).

These solutions indicate that for the smallest system, no matter how large the incentive for consensus p is, P_p can never be 1 [see Supplemental Material [35] for $P_p(p)$ with other values of G]. For larger systems P_p can show a sharp increase given enough attributes, as observed for $N = 11$ shown in Fig. 4(b). Otherwise, for instance for $G = 3$ or $G = 5$, paradise may not be likely for any value of p .

Invariant features.—When $p = 1/3$ different measures (e.g., probability P_p , or density ρ for both balanced and quasistationary states) are independent of the number of the attributes G . This observation has been confirmed in all numerical and analytical results for all network sizes. It is related to the fact that for $p = 1/3$ for all unbalanced triads all nodes and links are updated with the same probability. For this p the exact values for any N can be calculated only for some special cases, e.g., for $G = 1$: $\rho(G = 1) = 0.5$ and $P_p(G = 1) = 2^{-(N-1)}$. We have statistically confirmed that the above relations are valid for larger G (see Supplemental Material [35]).

Conclusions.—We developed a rigorous framework based on statistical physics that unifies the principles of homophily and structural balance and also provides an analytic treatment combining dyadic and triadic relationships. Rather than manipulating the polarity of links, as in most previous works on structural balance, we consider that link weights are a consequence of underlying attributes of nodes. This captures the fundamental perspective that agents have preferences, and also embeds our system in a Hamming space giving a quantitative measure of similarity between agents, and finally reveals the interplay of homophily and structural balance. The basis of our ABLTD model dynamics are adjustments of attributes. The triadic desire to achieve structural balance causes changes in attributes where the dyadic edge-weight dynamics obey a Fokker-Plank equation. These changes are performed in order for agents to become more or less similar, which is motivated by the positive and negative social influence, respectively [39]. The latter phenomenon is still under debate [40]. A recent experimental study shows that dyadic relations adapt towards structural balance when placed in triads with reciprocity also playing a role [41]. A phase transition from a quasistationary state to a paradise state can be observed in the ABLTD model and the nature of the transition depends on the exponent γ relating the number of attributes G and nodes N , where $G \sim N^\gamma$. Our study emphasizes the importance of incorporating attributes into structural balance theory and shows that homophily can impede a system from achieving balance and global cooperation.

Our analytic and numerical results indicate that the LTD and ABLTD models are equivalent in the limit $N, G \rightarrow \infty$ and $G > O(N^2)$. In such a case below $p < 0.5$ the system fluctuates around a quasistationary state. For $p > 0.5$ the system achieves the paradise state. When $G \leq O(N^2)$ the asymptotic results are different. For instance, when

$G < O(N^2)$, then the quasistationary state with equal number of balanced and unbalanced triads exists for all p .

An experimental analysis of homophily and structural balance would require proper datasets with time-varying data of agents' relations, opinions, and personal characteristics. With this one can estimate the possible fates of the system. As an example consider a small group of agents. Our model indicates that paradise is unlikely even with high eagerness towards consensus (parameter p). For a team (sports or industry) a common goal (a strong single attribute) may be sufficient in achieving a paradise state otherwise a leader may need interventions to create bonding relations and prevent division into separate subgroups, especially for large numbers of attributes [42]. Results from our model can explain why structural balance is not observed in some experiments over large social networks [43–45]. It may be the outcome from internal features of the network itself. The state without balance is also the natural state, as it is shown in our model for a wide range of node and attribute values. Incorporating susceptible and influential agents [46] into our triadic updating scheme, as well as zealots [42], would also be of interest.

Our work reveals the competing tension between homophily and structural balance and the importance of accounting for node attributes, especially when the number of the attributes is small, which we believe is the most common real-world scenario.

This research has received funding as RENOIR Project from the European Unions Horizon 2020 research and innovation programme under the Marie Skłodowska-Curie Grant Agreement No. 691152, by Ministry of Science and Higher Education (Poland), Grants No. W34/H2020/2016 and No. 329025/PnH/2016, by National Science Centre, Poland Grant No. 2015/19/B/ST6/02612, by POB Research Centre Cybersecurity and Data Science of Warsaw University of Technology within the Excellence Initiative Program - Research University (ID-UB), and by the U.S. Army Research Office MURI Grant No. W911NF-13-1-0340. K. B. and J. A. H. were partially supported by the Russian Science Foundation, Agreement No. 17-71-30029 with co-financing of the Bank Saint Petersburg.

*rmdsouza@ucdavis.edu

- [1] C. Castellano, S. Fortunato, and V. Loreto, *Rev. Mod. Phys.* **81**, 591 (2009).
- [2] A. T. Hartnett, E. Schertzer, S. A. Levin, and I. D. Couzin, *Phys. Rev. Lett.* **116**, 038701 (2016).
- [3] H. S. Sugiarto, J. S. Lansing, N. N. Chung, C. H. Lai, S. A. Cheong, and L. Y. Chew, *Phys. Rev. Lett.* **118**, 208301 (2017).
- [4] P. Jensen, T. Matreux, J. Cambe, H. Larralde, and E. Bertin, *Phys. Rev. Lett.* **120**, 208301 (2018).
- [5] F. Baumann, P. Lorenz-Spreen, I. M. Sokolov, and M. Starnini, *Phys. Rev. Lett.* **124**, 048301 (2020).

- [6] C. Merzel and J. D’Afflitti, *Am. J. Public Health* **93**, 557 (2003).
- [7] J. J. Bavel *et al.*, *Nat. Hum. Behav.* **4**, 460 (2020).
- [8] J. Yap and N. Harrigan, *Soc. Networks* **40**, 103 (2015).
- [9] F. Heider, *The Psychology of Interpersonal Relations* (John Wiley & Sons Inc., 1958), <https://psycnet.apa.org/record/2004-21806-000>.
- [10] P. Bonacich and P. Lu, *Introduction to Mathematical Sociology* (Princeton University Press, Princeton, NJ, 2012).
- [11] D. Cartwright and F. Harary, *Psychol. Rev.* **63**, 277 (1956).
- [12] K. Kułakowski, P. Gawroński, and P. Gronek, *Int. J. Mod. Phys. C* **16**, 707 (2005).
- [13] T. Antal, P. L. Krapivsky, and S. Redner, *Phys. Rev. E* **72**, 036121 (2005).
- [14] S. A. Marvel, S. H. Strogatz, and J. M. Kleinberg, *Phys. Rev. Lett.* **103**, 198701 (2009).
- [15] S. A. Marvel, J. Kleinberg, R. D. Kleinberg, and S. H. Strogatz, *Proc. Natl. Acad. Sci. U.S.A.* **108**, 1771 (2011).
- [16] X. Zheng, D. Zeng, and F. Y. Wang, *Inf. Syst. Front.* **17**, 1077 (2015).
- [17] A. M. Belaza, K. Hoefman, J. Ryckebusch, A. Bramson, M. Van Den Heuvel, and K. Schoors, *PLoS One* **12**, e0183696 (2017).
- [18] P. J. Górski, K. Kułakowski, P. Gawroński, and J. A. Hołyst, *Sci. Rep.* **7**, 16047 (2017).
- [19] F. H. Stillinger and T. A. Weber, *Phys. Rev. B* **31**, 5262 (1985).
- [20] F. Huber and O. Gühne, *Phys. Rev. Lett.* **117**, 010403 (2016).
- [21] P. S. Skardal and A. Arenas, *Phys. Rev. Lett.* **122**, 248301 (2019).
- [22] E. Agliari, F. Alemanno, A. Barra, M. Centonze, and A. Fachechi, *Phys. Rev. Lett.* **124**, 028301 (2020).
- [23] Y. Chen, L. Chen, X. Sun, K. Zhang, J. Zhang, and P. Li, *Eur. Phys. J. B* **87**, 62 (2014).
- [24] A. Parravano, A. Andina-Díaz, and M. A. Meléndez-Jiménez, *PLoS One* **11**, e0164323 (2016).
- [25] P. Singh, S. Sreenivasan, B. K. Szymanski, and G. Korniss, *Phys. Rev. E* **93**, 042306 (2016).
- [26] D. S. Lee, C. S. Chang, and Y. Liu, *IEEE Trans. Comput. Soc. Syst.* **3**, 141 (2016).
- [27] H. Du, X. He, and M. W. Feldman, *Complexity* **21**, 497 (2016).
- [28] H. Deng, P. Abell, O. Engel, J. Wu, and Y. Tan, *Soc. Networks* **44**, 190 (2016).
- [29] M. Saeedian, N. Azimi-Tafreshi, G. R. Jafari, and J. Kertesz, *Phys. Rev. E* **95**, 022314 (2017).
- [30] Z. Gao and Y. Wang, *PLoS One* **13**, e0191941 (2018).
- [31] R. Axelrod, *J. Conflict Resolut.* **41**, 203 (1997).
- [32] G. Deffuant, D. Neau, F. Amblard, and G. Weisbuch, *Adv. Complex Syst.* **03**, 87 (2000).
- [33] J. A. Rambaran, J. K. Dijkstra, A. Munniksma, and A. H. Cillessen, *Soc. Networks* **43**, 162 (2015).
- [34] A. Nigam, K. Shin, A. Bahulkar, B. Hooi, D. Hachen, B. K. Szymanski, C. Faloutsos, and N. V. Chawla, in *Machine Learning and Knowledge Discovery in Databases. ECML PKDD 2018*, edited by M. Berlingerio, F. Bonchi, T. Gärtner, N. Hurley, and G. Ifrim, Lecture Notes in Computer Science Vol. 11052 (Springer, Cham, 2019), https://link.springer.com/chapter/10.1007/978-3-030-10928-8_8.
- [35] See Supplemental Material at <http://link.aps.org/supplemental/10.1103/PhysRevLett.125.078302> for detailed mathematical justifications of analytical analysis and additional numerical results showing the consequences of the applied model, which includes Refs. [36–38].
- [36] E. Ben-Naim, P. L. Krapivsky, and S. Redner, *Fundamental Kinetic Processes* (Boston University, Boston, MA, 2008).
- [37] E. A. Codling, M. J. Plank, and S. Benhamou, *J. R. Soc. Interface* **5**, 813 (2008).
- [38] H. Risken, in *The Fokker-Planck Equation* (Springer, New York, 1996).
- [39] A. Flache, M. Mäs, T. Feliciani, E. Chattoe-Brown, G. Deffuant, S. Huet, and J. Lorenz, *J. Artif. Soc. Soc. Simul.* **20**, 2 (2017).
- [40] K. Takács, A. Flache, and M. Mäs, *PLoS One* **11**, 1 (2016).
- [41] Y.-S. Chiang and L. Tao, *Soc. Networks* **56**, 1 (2019).
- [42] A. Waagen, G. Verma, K. Chan, A. Swami, and R. M. D’Souza, *Phys. Rev. E* **91**, 022811 (2015).
- [43] J. Leskovec, D. Huttenlocher, and J. Kleinberg, in *Proceedings of the 28th International Conference on Human Factors in Computing Sys—CHI ’10* (ACM Press, New York, 2010), p. 1361, <https://dl.acm.org/doi/10.1145/1753326.1753532>.
- [44] J. Leskovec, D. Huttenlocher, and J. Kleinberg, *International World Wide Web Conference* (ACM Press, New York, 2010), p. 641, <https://dl.acm.org/doi/10.1145/1772690.1772756>.
- [45] M. Szell, R. Lambiotte, and S. Thurner, *Proc. Natl. Acad. Sci. U.S.A.* **107**, 13636 (2010).
- [46] N. N. Chung, L. Y. Chew, W. Chen, R. M. D’Souza, and C. H. Lai, *Phys. Rev. Research* **1**, 033125 (2019).